Journal of Power Sources 247 (2014) 883–889

Contents lists available at ScienceDirect

Journal of Power Sources

journal homepage: www.elsevier.com/locate/jpowsour

Composite anodes based on nanotube titanium oxide from electro-oxidation of Ti metal substrate☆

A. Pozio [a, *], M. Carewska [a], F. Mura [b], R. D'Amato [c], M. Falconieri [d], M. De Francesco [a], G.B. Appetecchi [a, *]

[a] UTRINN-IFC, ENEA (Agency for New Technologies, Energy and Sustainable Economic Development), Via Anguillarese 301, Rome 00123, Italy
[b] Department of Fundamental and Applied Science for Engineering, University of Rome, "La Sapienza", Via Antonio Scarpa 14, 00185 Rome, Italy
[c] UTAPRAD-MNF, ENEA, Via Enrico Fermi 45, 00044 Frascati, Rome, Italy
[d] UTAPRAD, ENEA, Via Anguillarese 301, 00123 Rome, Italy

HIGHLIGHTS

- Nanotube TiO_2 as anode material for lithium batteries was electrosynthesized from Ti metal.
- Good performance shown by electronic conductor-free nanotube TiO_2 anodes.
- Superior performance with respect to commercial TiO_2 and TiO_2 from laser pyrolysis.

ARTICLE INFO

Article history:
Received 29 April 2013
Received in revised form
20 August 2013
Accepted 2 September 2013
Available online 11 September 2013

Keywords:
Titanium oxide
Nanotubes
Electrosynthesis
Composite anodes
Lithium batteries

ABSTRACT

In this manuscript is reported an investigation on lithium-ion battery composite anodes based on nanotube titanium oxide active material obtained from electrochemical oxidation of titanium metal substrates. Nanotube TiO_2 showed a good nominal capacity, particularly taking into account that no electronic conductive additive as well as no binder was incorporated into the TiO_2 material. The performance of nanotube titanium oxide anode tapes was compared with that of electrodes based on TiO_2 both commercially available and obtained from laser pyrolysis. Cycling tests have indicated that the anodes based on electrosynthesized nanotube TiO_2 exhibit the best performance in terms of capacity values and rate capability in combination with very good capacity retention and coulombic efficiency leveling 100% even at high rates.

1. Introduction

Rechargeable lithium batteries are excellent candidates for the next generation power sources [1,2] because of their high gravimetric and volumetric energy with respect to other cell chemistries. The lithium-ion battery technology is based on the use of electrode materials able to reversibly intercalate Li^+ cations, e.g., a lithium transition metal oxide (LiMO) is used for the positive electrode (cathode) whereas a carbonaceous active material (generally graphite) is used for the negative electrode (anode). However, the performance of graphite anodes strongly depends on the stability of the passive layer (SEI), formed by the products resulting from the electrochemical reaction with the electrolyte during the first charge of the battery, at electrolyte/anode interface [1,2]. In addition, lithiated graphite electrode is strongly reducing, as it operates close to the potential of Li metal. The interface between lithiated graphite and the electrolyte is stable only because of the presence of SEI [3,4]. Therefore, eventual breaking (due to overheating and/or overcharging of the battery) of SEI is not welcome since it leads to electrochemical device failure with consequent fire and/or explosion [3,4].

Alternative anode materials are currently under worldwide investigation for replacing the graphite electrode. Among these, titanium oxide (TiO_2) results much safer than graphite as anode

* Corresponding authors.
E-mail addresses: alfonso.pozio@enea.it (A. Pozio), gianni.appetecchi@enea.it (G.B. Appetecchi).

0378-7753/$ – see front matter © 2013 Elsevier B.V. All rights reserved.
http://dx.doi.org/10.1016/j.jpowsour.2013.09.003

material since no growth passive layer occurs (or is stringently required) at interface with the electrolyte [5]. The adoption of titanium oxide is due to its *zero* strain structure during the intercalation process, this leading to an exceptional cycling stability [5]. In addition, TiO_2 exhibits several advantages as large capacity, high cycling stability (e.g., the material is able to operate within the electrochemical stability window of the electrolyte), very flat charge and discharge plateaus, coulombic efficiency close to 100%, low cost and environmental impact. Titanium oxide was initially investigated in the 80's by Ohzuku et al. [6] and Zachau-Christiansen et al. [7] and, successively, by Kavan et al. [8] who have recorded a nominal capacity equal to 168 mA h g^{-1} in microsize TiO_2. Higher capacity values in combination with good rate performance were exhibited from nanoscale TiO_2, due to additional lithiation shown from $LiTiO_2$, as reported by Gao et al. [9], Li et al. [10], Xu et al. [11], Bao et al. [12] and Bresser et al. [13]. Capacity values exceeding 200 mA h g^{-1} were also obtained in commercial nanocrystalline titanium oxide material, even if at low current rates, by Moretti et al. [14].

However, TiO_2 shows poor electronic conduction, thus needing to be careful coated with an appropriate electron conductor (carbon) for use in practical devices. At the same time, large efforts are devoted to synthesize titanium oxide materials having nanometric particle size. Among these, nanotube TiO_2 represents an appealing compound, resulting one of the most investigated nanoscale active materials for lithium battery systems [15].

Nanosize TiO_2 can be prepared through different procedures and, among them, electrochemical methods as proposed by Macak et al. [16,17]. A few of us have previously reported a new electrochemical route for obtaining well-aligned, regular TiO_2 nanotubes from a titanium metal substrate [18,19]. In the present manuscript we present the results of a physicochemical and electrochemical investigation performed on composite anodes based on electrosynthesized nanotube titanium oxide as the active material. The electrochemical performance of composite nanotube titanium oxide anode tapes was compared with that of Ti-supported, carbon-free, TiO_2 nanotubes and of electrodes based both on TiO_2 both commercially available and obtained in lab-scale from laser pyrolysis.

2. Experimental

2.1. Electrosynthesis of titanium oxide

Titanium oxide nanotubes were prepared through electrochemical oxidation of titanium metal (provided from Titania) discs having diameter and thickness equal to 15 mm–0.5 mm, respectively. Preliminary results were reported elsewhere [18,19]. The samples, previously encapsulated in a PTFE mount, exhibit electrochemical active areas equal to 1 cm^2. The growth of TiO_2 nanotubes onto the Ti° substrate surface was allowed through a five consecutive step procedure route:

a) *Chemical etching of Ti° surface*: the titanium disc samples were undergone to chemical etching in a HF (provided from Carlo Erba), 5 vol.%, and HNO_3 (Air Products), 15 vol.%, water solution. Such a treatment allows removing the passive layer and impurities onto the titanium surface.
b) *Preliminary galvanostatic oxidation*: this step allows obtaining a uniform and homogeneous TiO_2 layer onto the titanium coin. The Ti° disc, used as the working electrode, was coupled with a Pt° counter electrode in a two-electrode cell containing a 1 M KOH (Carlo Erba) aqueous electrolyte. Successively, a current density equal to 1 mA cm^2 was applied for 3 min (25 °C) by a Solartron 1286 Electrochemical Interface.
c) *Potentiostatic oxidation*: The growth of the TiO_2 nano-tubes was promoted through potentiostatic oxidation of the Ti° electrode (working), coupled with a Pt° counter electrode, in ethylene glycol (Ashland) electrolyte containing de-ionized water (1 wt.%) and NH_4F (Carlo Erba, 0.2 wt.%). A voltage equal to 60 V has been applying for 3 h by a potentiostat/galvanostat Aldrich PS251-2. The current flow through the cell was detected by a potentiometer/galvanometer Keithley 2000 and recorded (as a function of the time) by a Madge-Tech Volt101 equipment in series with a 300 Ω resistance (Leeds and Northrup).
d) *Vacuum drying*: The samples obtained from step (*c*) were vacuum dried at 90 °C for 3 h to remove the residual water from the oxidation steps.
e) *Thermal annealing*: Finally, the vacuum dried samples were thermally annealed at 580 °C (heating rate equal to 2 °C min^{-1}) for 1 h into a Lenton oven in order to crystallize the TiO_2 nanotubes.

The electrosynthesis preparation route described above allowed to obtain self-standing, nanotube TiO_2 anodes (Fig. 1, panel A) having an active material mass loading ranging from 1 mg cm^{-2} to about 3.5 mg cm^{-2}.

2.2. Titanium oxide prepared through laser pyrolysis

Nanoscale (e.g., particle size ranging from 20 to 30 nm) titanium oxide (mainly composed of the crystalline anatase phase as shown by Raman measurements) was synthesized through a laser pyrolysis route, performed using titanium tetra-isopropoxide as the

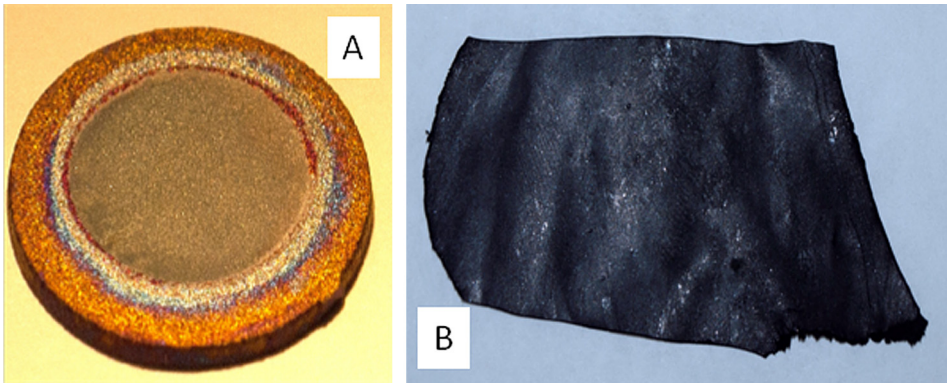

Fig. 1. Picture of a nanotube TiO_2 anode supported onto a Ti° metal substrate (panel A) and a composite anode tape (panel B) based on nanotube TiO_2 as the active material.

precursor and reported in details elsewhere [20]. The TiO_2 particles were found (by Dynamic Light Scattering measurements) to form aggregates having a hydrodynamic radius around 180 nm.

2.3. Commercial titanium oxide

The commercial TiO_2, investigated for comparison purpose, was purchased from Evonik (P25). This titanium oxide material, constituted by 80% of anatase phase and 20% of rutile phase, is an uncoated, crystalline, white powder, whose primary article size ranges from 25 to 30 nm [21]. However, particle aggregates around 100 nm in size are found, corresponding to a surface area of 50 $m^2\ g^{-1}$.

2.4. SEM analysis

The morphological structure of TiO_2 materials was investigated through SEM analysis using a FESEM Zeiss Auriga 405 with the following values of extraction potential and *working distance* equal to 1.5 keV and 5.4 mm, respectively. The composition analysis was performed using an EDX (Energy Dispersive X-Ray) Bruker Quantax detector.

2.5. TGA measurements

Thermal stability measurements were run using a Q600 SDT TG-DTA differential scanning calorimeter in synthetic air flow (100 ml min^{-1}) to avoid contamination with external. High purity aluminum oxide was used as the reference material. The TiO_2 samples (weight ranging from 10 to 12 mg), stored and handled within an atmosphere-controlled (R.H. < 0.1%) dry-room, were loaded in platinum pans (cross section equal to a 0.32 cm^2). Heating scans (10 °C min^{-1}) were run on the sample under test from room temperature to 600 °C.

2.6. Preparation of composite anodes

The titanium oxide materials, obtained both through electrosynthesis and laser pyrolysis routes and commercially available (Evonik), were used for preparing composite anode tapes. All anode components were previously dried under vacuum overnight at 120 °C. The active material (TiO_2) and the electronic conductor (Super-P carbon, MMM) were intimately mixed in an agate mortar for at least 10 min. This step allows a suitable carbon coating onto the titanium oxide particles and, therefore, good electronic conduction through the anode tape. The polymer binder (PTFE) was added to the TiO_2-carbon blend and mixed for at least 10 min to obtain a plastic-like material. The last was cold-calendered to obtain homogeneous anode tapes (having a thickness around 70 μm) from which coins, having a diameter equal to 3 mm (active area equal to about 0.2 cm^2) and a capacity ranging from 0.6 to 0.7 mA h cm^{-2} (taking into account a TiO_2 specific capacity equal to 168 mA h g^{-1}) were punched. Finally, the anodes (having the following weight composition: TiO_2 60%; carbon 25%; PTFE 15%) were dried under vacuum (<10^{-3} mbar) at 100 °C for at least 15 h. The preparation route was performed within the dry-room. Panel B of Fig. 1 reports a picture of a composite anode tape upon calendaring step.

2.7. Electrochemical tests

The electrochemical performance of TiO_2 nanotube (supported onto Ti° substrate) anodes (active area equal to 1.54 cm^2) as well as of the composite electrodes (steel as the current collector) was investigated in Li/TiO_2, T-shaped (polyethylene-made) cells where a lithium metal coin is the counter electrode and the electrolyte is a 1 M $LiPF_6$ in EC/DEC (1:1 in weight) solution embedded in a glass fiber disc. The cells, manufactured in the dry-room, were characterized through consecutive discharge/charge cycles run (at 100% of deep of discharge, DoD) at different current rates (from C/10 through 3C) within the 1.4–2.5 V voltage range. The measurements were performed by a multichannel Maccor 4000 battery tester within the dry-room at 20 °C. The electrochemical performance was evaluated in terms of specific capacity, rate capability, capacity retention, cyclability and coulombic efficiency.

3. Results and discussion

The physicochemical properties of titanium oxide are correlated to the crystalline content and morphological structure of the TiO_2 anode material, which displays three different phases (Fig. 2) denominated anatase (tetragonal), rutile (tetragonal) and brookite (orthorhombic) [5,15]. The anatase phase is preferred as anodic active material for lithium batteries because its higher capability to reversibly intercalate lithium cations within the reticular lattice. The crystallization process of the anatase phase occurs at 280 °C, starting from the nano-tube core to progressively moving towards the external regions. Conversely, the most external layer is hold in the amorphous state. This process was found to be independent on the reaction atmosphere. The temperature increase promotes the growth of crystalline nuclei. At 430 °C (in O_2 atmosphere) formation of rutile phase starts to occur at titanium oxide nanotube/titanium metal interface but, however, without affecting the crystallization of the TiO_2-anatase nanotubes. Therefore, an optimal thermal treatment has to be performed in a dry oxygen atmosphere at 580 °C to avoid an uncontrolled and unwelcome growth of the rutile phase, this resulting in cracking of the Ti° oxide nanotube layer or detachment from the titanium substrate [15–17].

The XRD pattern of nanotube TiO_2 (red trace), obtained through electrosynthesis route, is depicted in Fig. 3. From comparison with the Ti° substrate pattern (black trace), all features typical of the titanium metal are observed. However, a few peaks, ascribable to titanium oxide material (labeled with asterisk), can be recognized [22]. The results indicate high degree of crystalline phase in the nanotube constituted by TiO_2, suggesting that the electrosynthesis route does not lead to any amorphous region content. The

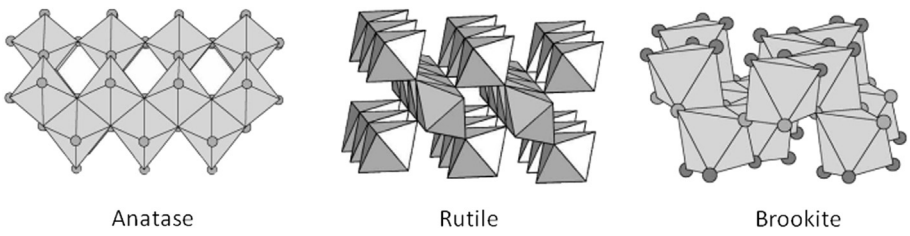

Fig. 2. Lattice structure of different TiO_2 active material phases.

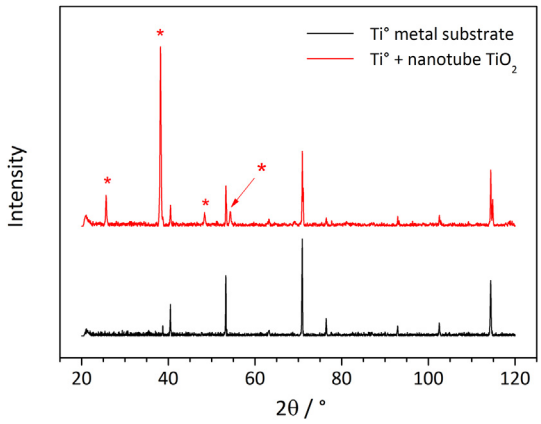

Fig. 3. XRD pattern of nanotube TiO_2 (red trace) obtained through electrosynthesis route. The pattern of the Ti° substrate (black trace) is reported for comparison purpose. (For interpretation of the references to colour in this figure legend, the reader is referred to the web version of this article.)

crystalline structure of laser pyrolysis and commercial TiO_2 was confirmed by XRD measurements previously reported in literature [21,23,24].

The results of the SEM analysis are reported in Figs. 4 and 5. The formation of titanium oxide nanotubes (obtained by electrosynthesis) onto the Ti° substrate is clearly highlighted by the top view reported in panel A of Fig. 4. It is to note the TiO_2 nanotubes seem to be interconnected on their top side whereas Fig. 4A shows that they are separated with respect to each other. This is due to the presence of a TiO_2 layer (on the nanotube top side) not fully removed by the chemical etching in HNO_3/HF, leading to a decrease of the top cross-section of the nanotubes [25]. Panel B of Fig. 4 shows a bottom view of the TiO_2 nanotubes which, as expected, are closed on their inferior side [25]. The nanoscale of the TiO_2 tubes, which appear well aligned and very similar in size and shape, is also confirmed, e.g., about 400 nm in height and 100 nm in diameter as also reported by Schmuki and co-workers [26]. Fig. 5 depicted images concerning anode tapes based on TiO_2 obtained through different synthesis routes compared with commercial titanium oxide. The anodes show a rather uniform, nanoscale particle size even if microscale clusters are observed. A homogeneous distribution of porosity is also detected.

Thermogravimetrical (TGA) measurements were performed on TiO_2 material obtained through laser pyrolysis. This technique allows to obtain titanium oxide coated by carbon particles, generally not welcome. Conversely, this issue result of interest for applications in lithium batteries since the poor electronic conduction of electrode active materials. Therefore, a good electron conductor has to be incorporated into electrodes in order to assure high performance in battery. Fig. 6 reports the TGA trace, recorded in synthetic air atmosphere, and its derived referred to laser pyrolysis titanium oxide. A progressive decrease in weight is observed up to 400 °C (5% with respect to the initial mass) due to the loss of humidity adsorbed from external, e.g., up to 100 °C, and to carbon particle burning, which occurs above 100 °C. Therefore, the carbon content within the TiO_2 obtained through laser pyrolysis may be approximately estimated about 5% in weight. At temperatures higher than 400 °C a faster sample weight loss is detected, clearly evidenced from the feature of the derived curve. Above 450 °C a slower weight loss suggests the formation of thermally stable compounds.

The intercalation process of lithium cations within titanium oxide active material occurs according to the reaction:

$$TiO_2 + xLi^+ + xe^- \leftrightarrow Li_xTiO_2 \quad (1)$$

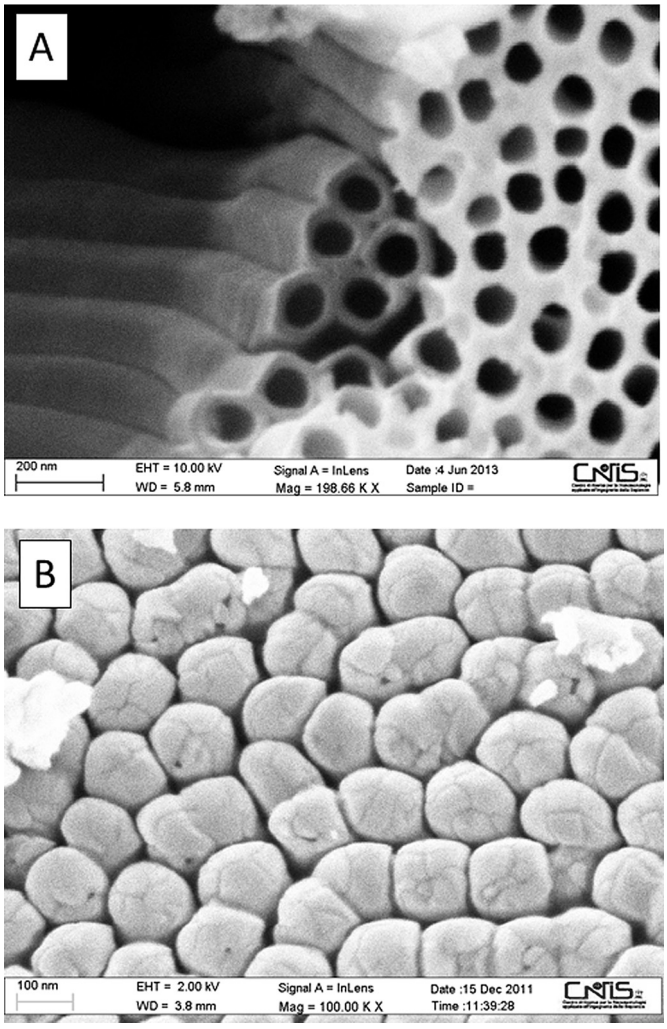

Fig. 4. SEM images of TiO_2 nanotubes obtained through electrosynthesis route. Panel A: top view; panel B: bottom view.

where 0.5 equivalent of Li^+ are reversibly intercalated at a nominal voltage of 1.78 vs. Li/Li^+, corresponding to a nominal capacity equal to 168 mA h g^{-1} (anatase phase) [5,15]. Fig. 7 reported voltage vs. capacity profiles (panel A) and the capacity behavior (panel B) at different current rates for nanotube TiO_2 anodes, supported onto Ti° substrate, obtained through electrosynthesis route. Well-defined plateaus (panel A), typical of titanium oxide materials [15], are observed around 1.8 V (intercalation) and about 1.9 V (de-intercalation) along the almost whole discharge and charge half-cycles, respectively, this confirming the goodness of the electrochemical synthesis. For instance, the peculiarity to deliver stable voltage value during the discharge step is welcome in battery systems. The increase of the current rate leads to progressively less pronounced voltage plateaus due to diffusive phenomena through the TiO_2 anode and the electrolyte [27]. The ohmic drop was found to raise from 250 mV to about 600 mV on passing from C/10 to 3C (e.g., corresponding to an increase in current density equal to thirty times). Above 1C less than 30% of the nominal capacity is delivered (panel B of Fig. 7), which is reduced down to 16% at 3C (Table 1). Even if these do not represent exceptional (or lower) capacity values with respect to analogous TiO_2 materials previously reported in literature, it is worthy to note that no electronic conductor was incorporated into TiO_2 nanotubes, despite it is well known that electrode active materials, particularly such as TiO_2,

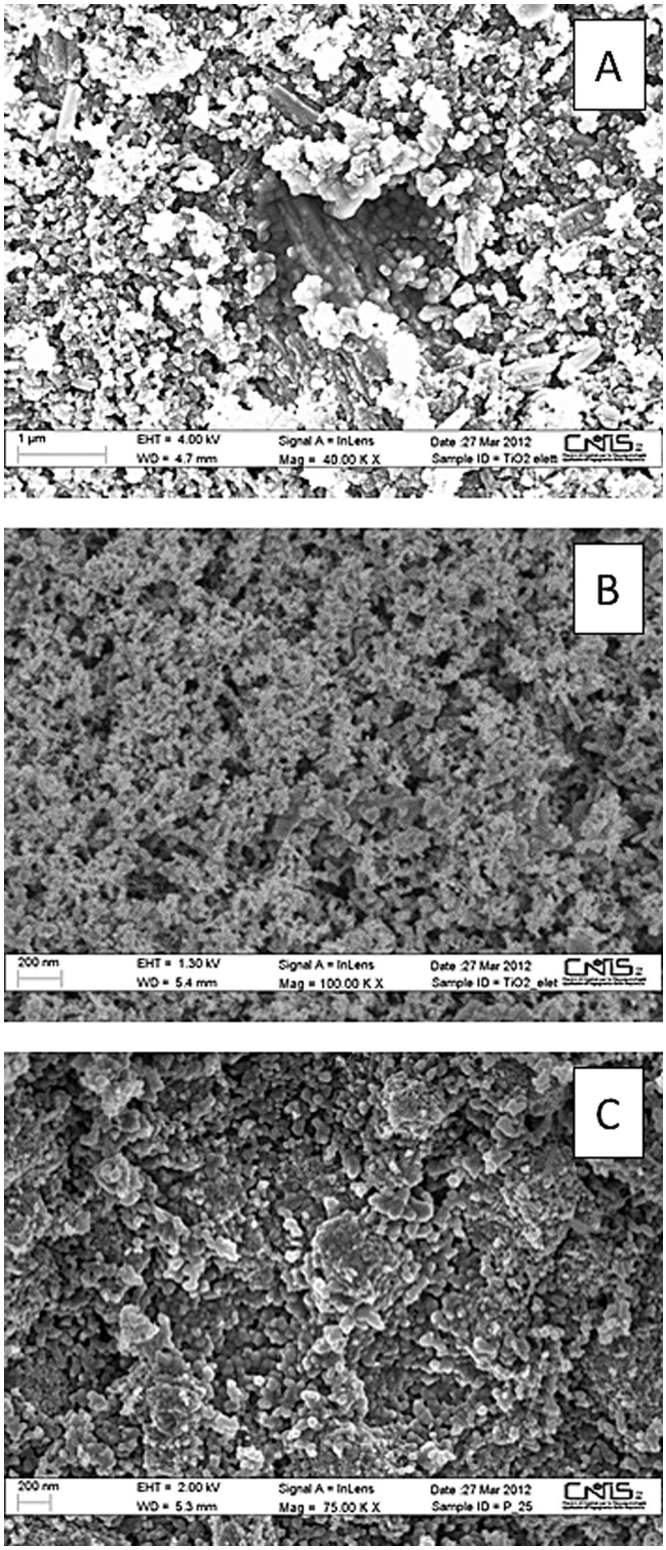

Fig. 5. SEM images of composite anode tapes based on TiO_2 obtained through different procedure routes: panel A (electrosynthesis); panel B (laser pyrolysis); panel C (commercial). The magnification values are reported in the panels.

stringently need high electron conduction additives in order to give good performance especially at high rates [5–15]. Therefore, the capacity values delivered from TiO_2 nanotubes, particularly at high current rates, have to be considered among the largest, if not the

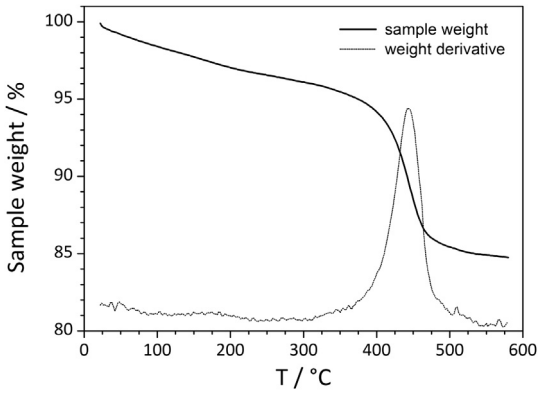

Fig. 6. TGA trace its derived of TiO_2 obtained through laser pyrolysis. Scan rate: 10 °C min^{-1}.

largest ones, concerning electronic conductor-free active materials [28]. This interesting performance is to be ascribed to the very short pathway of Li^+ cations (and electrons) through the TiO_2 nanotubes. In addition, it is to note a very limited irreversible capacity at the 1st discharge/charge cycle in combination with a coulombic efficiency leveling 100% even at high current rates.

The results of the cycling tests performed on the composite anode tapes, based on TiO_2 obtained through different procedure routes, are compared in Figs. 8 and 9. The voltage vs. capacity profiles, recorded at different current rates, are shown in Fig. 8 (panels from A through C), which exhibits well-defined plateau around 1.8 V and 1.9 V along the whole duration of the discharge and charge step [15], respectively, particularly for the nanotube TiO_2 anode tapes (panel A). It is well known that the ability to deliver energy at stable voltage values is an appealing property for applications in battery systems. The increase in current density (from C/10 to 3C) results in progressively less pronounced voltage plateaus, likely ascribed to diffusive phenomena within the

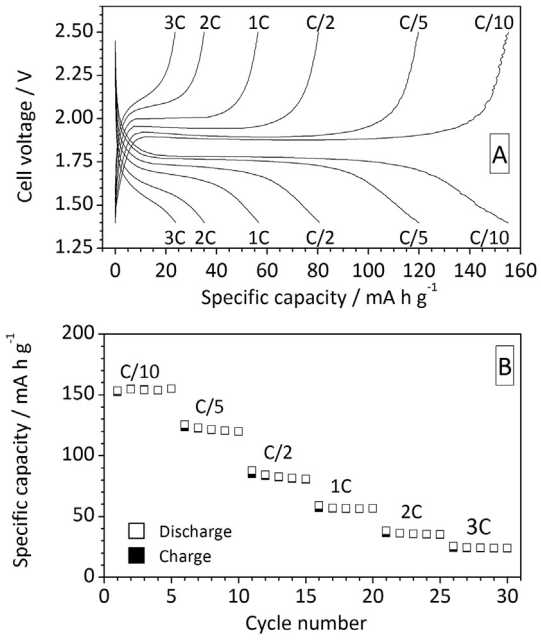

Fig. 7. Charge–discharge voltage/capacity profiles (panel A) and capacity evolution (panel B), recorded at different current rates, of nanotube TiO_2 anodes in $LiPF_6$(1 M)/EC:DEC(1:1 weight ratio) electrolyte. $T = 20$ °C.

Table 1
Specific capacity values delivered at different current rates from nanotube TiO_2 anodes in $LiPF_6$(1 M)/EC:DEC (1:1 weight ratio) electrolyte at 20 °C. The corresponding equivalent value of intercalated Li^+ cations per mole of TiO_2 was also reported.

Current rate	Specific capacity/mA h g^{-1}	Equivalent of Li^+ per mole of TiO_2
C/10	154	0.46
C/5	122	0.36
C/2	83	0.25
1C	57	0.17
2C	36	0.11
3C	24	0.07

electrode and electrolyte, but without any remarkable increase in ohmic drop.

The cycling performance, obtained at various current rates, is also reported in Fig. 9. The nanotube TiO_2 anode tapes (panel A) exhibit a nominal capacity equal to 166 mA h g^{-1}. Above 75% of the nominal capacity is delivered up to medium rates (e.g., 125 mA h g^{-1} at C/2), however, appreciable values are still recorded at high current rates (80 mA h g^{-1} and 60 mA h g^{-1} at 2C and 3C, respectively). Therefore, about 36% of the nominal capacity, obtained at C/10, is discharged at 3C. This behavior may be addressed to the relatively fast kinetics of the Li^+ intercalation process within the TiO_2 nanotube. The anode tapes based on TiO_2 prepared by laser pyrolysis (panels B of Figs. 8 and 9) exhibit large capacities only at low medium rates, e.g., 123 mA h g^{-1} and 105 mA h g^{-1} are delivered at C/10 and C/5, respectively. At high current rates (>2C) less than 30 mA h g^{-1}, e.g., below 18% of the nominal capacity, are discharged. Finally, the anodes based on commercial TiO_2, reported for comparison purpose in panels C of Figs. 8 and 9, approach at

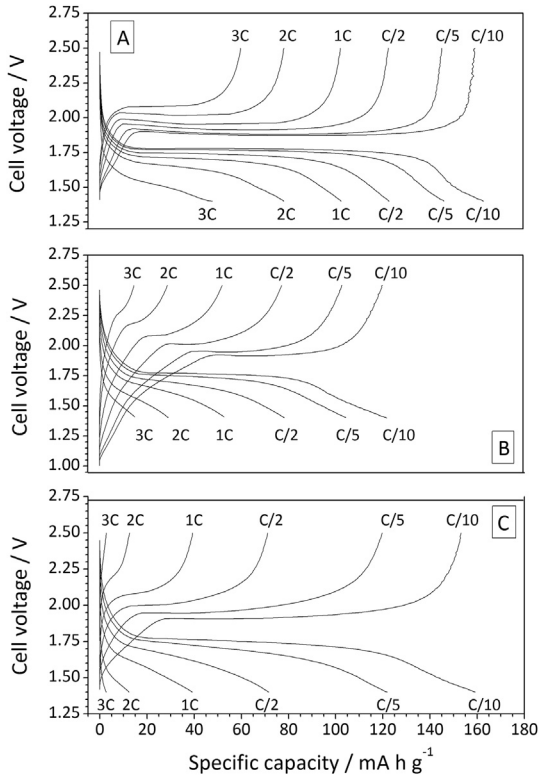

Fig. 8. Charge–discharge voltage/capacity profiles, recorded at different current rates, of TiO_2 composite anodes in $LiPF_6$(1 M)/EC:DEC(1:1 weight ratio) electrolyte at 20 °C. Panel A: nanotube TiO_2 from electrosynthesis; panel B: TiO_2 from laser pyrolysis; panel C: commercial TiO_2.

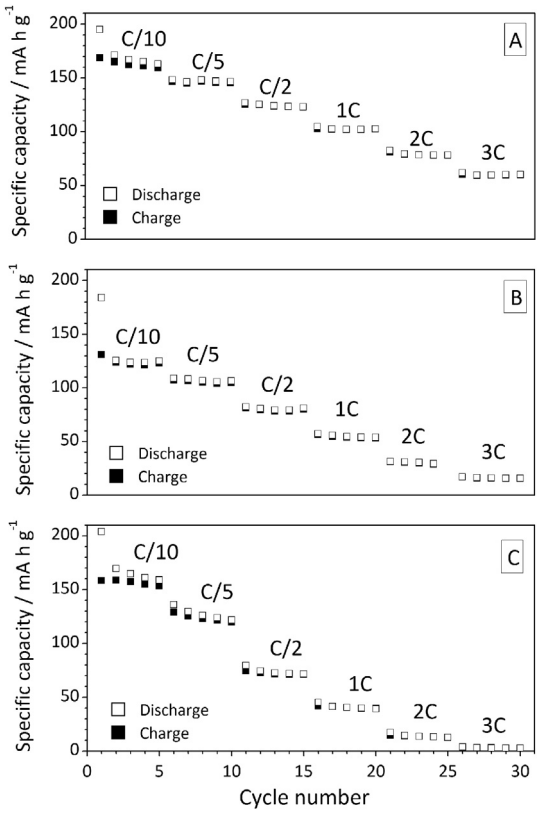

Fig. 9. Capacity evolution, recorded at different current rates, of TiO_2 composite anodes in $LiPF_6$(1 M)/EC:DEC(1:1 weight ratio) electrolyte at 20 °C. Panel A: nanotube TiO_2 from electrosynthesis; panel B: TiO_2 from laser pyrolysis; panel C: commercial TiO_2.

low-medium rates (C/5–C/10) the capacity values exhibited by the TiO_2 nanotubes (panels A in Figs. 8 and 9). Above 95% (160 mA h g^{-1}) and 73% (123 mA h g^{-1}) of the nominal capacity is delivered at C/10 and C/5, respectively, whereas further increases of the current density result in more marked decrease in capacity, approaching the values displayed by the anodes based on TiO_2 from laser pyrolysis (panel B). The results reported in Fig. 9 also evidence a high capacity retention (at 100% of DOD) even at high current rates in conjunction with a coulombic efficiency close to 100%. The nanotube TiO_2 composite anodes were found to exhibit the lowest

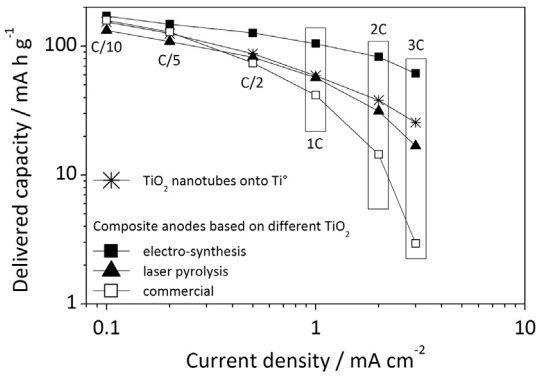

Fig. 10. Delivered capacity vs. current density dependence of composite anodes based on TiO_2 prepared according to different procedure route (see legend). The data referred to nanotube TiO_2 anodes (supported onto Ti° metal substrate) are depicted for comparison purposes. The current rates are also reported. $T = 20$ °C.

irreversible capacity (13.6%) during the 1st cycle with respect to the electrode based on titanium oxide material obtained through laser pyrolysis (about 29%) and on commercial titanium oxide (23.2%). This behavior suggests that the intercalation process of the lithium cation occurs without any appreciable stress of the Ti–O lattice, especially for electrosynthesized nanotube TiO_2.

Fig. 10 plots the discharge capacity vs. current density dependence for composite anode tapes based on TiO_2 prepared through different procedure routes. The data referred to nanotube TiO_2 anodes (star markers), directly obtained through electrosynthesis of titanium metal substrates, are reported for comparison purpose. Once more, the results highlight how the composite anodes based on electrosynthesized nanotube TiO_2 (solid squares) exhibit the best performance in terms of capacity values and rate capability. Titanium oxide anodes from laser pyrolysis (solid triangles) shows remarkable lower capacities whereas commercial TiO_2 anodes (open squares) deliver high performance only at low-medium current rates ($\leq$0.4 mA cm^{-2}). Therefore, the electrochemical route results appealing in order to synthesize TiO_2 anode materials with high capacity and cyclability even at high rates.

4. Conclusions

Nanotube titanium oxide as anode material for lithium-ion batteries was synthesized through electrochemical oxidation of Ti° substrates. This procedure route allowed the growth of very regular, well-aligned, TiO_2 nanotubes onto the titanium metal, as confirmed by SEM analysis, showing a nominal capacity of 168 mA h g^{-1}, which reduces down to 30% at 1C. Even if these results are not excellent (or, sometimes, lower), especially if compared with analogous titanium oxide materials previously reported in literature, it is worthy taking into account, however, that no electronic conductive additive as well as no binder was incorporated into the TiO_2 material. This issue, in combination with the simplicity of the electrochemical synthesis route, makes this active material appealing for lithium-ion battery systems. However, further work is in progress in our laboratory with the aim to improve the performance of the TiO_2 nanotubes.

Nanotube titanium oxide was used as the active material for manufacturing composite anodes which were compared with the electrodes based on TiO_2 both commercially available and obtained from laser pyrolysis. Electrosynthesized nanotube TiO_2 exhibited the best performance in terms of capacity values and rate capability in combination with good capacity retention and coulombic efficiency leveling 100% even at high rates. For instance, a nominal capacity (166 mA h g^{-1}) is exhibited (C/10) and above 125 mA h g^{-1} are delivered at C/2. Also, 80 mA h g^{-1} and 60 mA h g^{-1} are still recorded at 2C and 3C, respectively.

Acknowledgment

The financial support of the Italian Ministry of Economic Development (MSE), within the Program Agreement ENEA-MSE on Electric System Research, is kindly acknowledged.

References

[1] G. Pistoia (Ed.), Lithium Batteries, New Materials, Developments and Perspectives, Industrial Chemistry Library, Elsevier, 1995.
[2] J.M. Tarascon, M. Armand, Nature 414 (2001) 359.
[3] R. Spotnitz, J. Franklin, J. Power Sources 113 (2003) 81.
[4] H. Yang, S. Amiruddin, H.J. Bang, Y.K. Sun, J. Prakash, J. Ind. Eng. Chem. 12 (2006) 12.
[5] K. Kawamura, T. Umegaki, H. Naito, Z. Takehara, T. Yao, J. Appl. Electrochem. 31 (2001) 73.
[6] T. Ohzuku, T. Kodama, T. Hirai, J. Power Sources 14 (1985) 153.
[7] B. Zachau-Christiansen, K. West, T. Jacobsen, S. Atlung, Solid State Ionics 28–30 (1988) 1176.
[8] L. Kavan, M. Grätzel, S.E. Gilbert, C. Klemenz, H.J. Scheel, J. Am. Chem. Soc. 118 (1996) 6716.
[9] X. Gao, H. Zhu, G. Pan, S. Ye, Y. Lan, F. Wu, D. Song, J. Phys. Chem. B 108 (2004) 2868.
[10] J. Li, Z. Tang, Z. Zhang, Electrochem. Solid State Lett. 8 (2005) A316.
[11] J. Xu, C. Jia, B. Cao, W.F. Zhang, Electrochim. Acta 52 (2007) 8044.
[12] S.-J. Bao, Q.-L. Bao, C.-M. Li, Zhi-Li Dong, Electrochem. Commun. 9 (2007) 1233.
[13] D. Bresser, E. Paillard, E. Binetti, S. Krueger, M. Striccoli, M. Winter, S. Passerini, J. Power Sources 206 (2012) 301.
[14] A. Moretti, G.-T. Kim, D. Bresser, K. Renger, E. Paillard, R. Marassi, M. Winter, S. Passerini, J. Power Sources 221 (2013) 419.
[15] J.M. Macak, H. Tsuchiya, L. Taveira, S. Aldabergerova, P. Schmuki, Angew. Chem. Int. Ed. 44 (2005) 7463.
[16] J.M. Macak, H. Tsuchiya, A. Ghicov, K. Yasuda, R. Hahn, S. Bauer, P. Schmuki, Curr. Opin. Solid State Mater. Sci. 11 (2007) 3.
[17] J.M. Macak, H. Hildebrand, U.M. Jahns, P. Schmuki, J. Electroanal. Chem. 621 (2008) 254.
[18] F. Mura, A. Masci, M. Pasquali, A. Pozio, Electrochim. Acta 54 (2009) 3794.
[19] F. Mura, A. Masci, M. Pasquali, A. Pozio, Electrochim. Acta 55 (2010) 2246.
[20] R. D'Amato, M. Falconieri, S. Gagliardi, E. Popovici, E. Serra, G. Terranova, E. Borsella, J. Anal. Appl. Pyrol. (2013) in press.
[21] V. Vamathevan, H. Tse, R. Amala, G. Low, S. McEvoy, Catal. Today 68 (2001) 201.
[22] J. Kasetsart, Nat. Sci. 42 (2008) 357.
[23] E. Borsella, S. Botti, L. Caneve, L. De Dominicis, R. Fantoni, Phys. Scr. 78 (2008) 58112.
[24] E. Borsella, S. Botti, S. Martelli. Trans. Tech. Publications, Mat. Sci. Forum 235–238 (1997) 236.
[25] K. Lu, Z. Tian, J.A. Geldmeier, Electrochim. Acta 56 (2011) 6014.
[26] S.P. Albu, A. Ghicov, J.M. Macak, P. Schmuki, Phys. Status Solidi RRL 1 (2007) R65.
[27] C.A. Vincent, B. Scrosati, Modern Batteries, an Introduction to Electrochemical Power Sources, second ed., Arnold, London, 1993.
[28] M. Carewska, G.B. Appetecchi, F. Cardellini, S. Passerini, Solid State Ionics 139 (2001) 211.